doi:10.3788/gzxb20144308.0823001

多参量可调谐的 Bragg 波导光栅滤波器设计

张爱玲,李玉祥

(天津理工大学 计算机与通信工程学院,天津市薄膜电子与通信器件重点实验室,天津 300384)

摘 要:为了解决基于光纤布喇格光栅和压电陶瓷结构的任意光脉冲整形器在动态调谐时存在不足的问题,提出并设计了一种波长、相位、幅度参量独立可调的 Bragg 波导光栅滤波器,以实现谐振波长及谐振波相位快速独立的线性调控.理论分析表明:波长和相位的理论调谐效率分别为 15.6 pm/V 和 0.2π/V,滤波器的输出光强度可以通过偏振旋转器控制.基于转移矩阵理论的仿真分析发现:该滤波器在蚀刻占空比为 1/2 时反射率最大,光栅长度为 10.869 mm,蚀刻深度大于 100 nm 时,可以获得 98.4%以上的反射率和大于 0.14 nm 的带宽;增大波长调谐电压会进一步降低滤波带宽.

关键词:光学滤波器;光学设计;动态光栅;铌酸锂;电光效应

中图分类号:TN256; TN202 **文献标识码**:A **文章编号**:1004-4213(2014)08-0823001-5

Design of Multi-Parameter Tunable Bragg Waveguide Grating Filter

ZHANG Ai-ling, LI Yu-xiang

(*Tianjin Key Laboratory of Film Electronics and Communication Devices, Communication Device and Technology Engineering Research Center, Tianjin University of Technology, Tianjin* 300384, *China*)

Abstract: In order to solve the problem of poor tuning performence of the optical arbitrary waveform generator based on fiber Bragg grating and piezoelectric transducer, a novel multi-parameter fast tunable Bragg grating filter on lithium niobate crystal was proposed. Theory analysis shows that its Bragg wavelength and corresponding phase is tunable in a linear way with wavelength tuning efficiency of 15.6 pm/V and phase tuning efficiency of 0.2 π/V, and the output light intensity of the filter is controlled by adjusting a polarization rotator also. Simulation results based on transfer matrix theory show that the maximum filtering reflectivity is achieved with the etching duty cycle 1/2, reflectivity more than 98.4% and bandwidth wider than 0.14 nm is obtained when etching depth is deeper than 100 nm on the condition of 10.87 mm grating length, and increasing the wavelength tuning voltage will further reduce the filter bandwidth.

Key words: Optical filters; Optical design; Dynamic grating; Lithium niobate; Electro-optic effect

OCIS Codes: 190.2055; 130.3730; 130.7408

0 Introduction

Tunable Bragg grating filter with narrow-band characteristic, which can be used as narrow bandwidth reflector[1], plays an important role in the field of high-speed optical communication networks. It mainly includes fiber grating filters and waveguide grating filters[2-3]. Compared to the slow tuning speed of fiber gratings, waveguide gratings have taken advantage of a variety of materials included inorganic crystals, polymers, semiconductors, etc, to produce various fast tunable devices[4-6]. Especially, tunable grating filters based on electro-optic effect have become an important research spot. A tunable waveguide Bragg grating on

Foundation item: The National Natural Science Foundation of China (No. 61377075)

First author: ZHANG Ai-ling (1973—), female, professor, Ph. D. degree, mainly focuses on optic fiber communication technology. Email:alzhang2012@163.com

Contact author: LI Yu-xiang (1986—), male, M. S. degree, mainly focuses on tunable Bragg waveguide gratings. Email:lyx411976807@163.com

Received: Nov. 12, 2013; **Accepted**: Jan. 16, 2014

polarized polymer was designed[7], which enable resonant wavelength rapid tuning based on the Electro-Optic (EO) effect of poled polymer. However, the EO polymer is sensitive to environment and easy depolarization. Lithium niobate ($LiNbO_3$: LN) as an EO material with a high EO coefficient has good optical transmission properties[8]. It has widely adopted in various fast tunable EO devices. A tunable Bragg filter with the wavelength tuning efficiency of 5pm/V on LN was reported in 2008[9]. The tuning speed of the filter is in the order of nanosecond. A tunable long-period grating based on LN was reported in 2010[10], which its transmittance is tunable by using crossed electrodes.

So far, the fast tunable grating filters reported recently can only achieve one parameter tuning, such as amplitude or wavelength. Multi-parameter tunable filter is required in the emerging Optical Arbitrary Waveform Generator (OAWG) technology in recent years[11]. In this paper, a multi-parametric tunable Bragg grating filter on LN is proposed. The Bragg wavelength and the corresponding phase of the filter can be tuned respectively, while the intensity of the filter can also be controlled independently.

1 Structure of the filter

The schematic structure of the designed filter is shown in Fig. 1. It is comprised of a polarization rotator, a Polarization Maintaining Optical Circulator (PMCIR) and a tunable waveguide grating. The structure of the tunable waveguide grating comprises wavelength control section and phase control section, which is shown in Fig. 2. A Bragg grating is etched on one end of the Annealed Proton Exchange (APE) single-mode waveguide on X-cut $LiNbO_3$ wafer. Coplanar flat electrodes are accordingly deposited on both sides of the grating and the APE waveguide, while there is a gap between the electrodes to ensure the electrodes work independently. In the structure, the objective wavelength, passing through the polarization rotator and the PMCIR, output from port 3 after reflected by the tunable waveguide grating. The polarization rotator is used to control the intensity of the reflected wave by adjusting its polarization direction. The electrodes pair A are used to control the reflective wavelength and the electrodes pair B are used to control the phase of corresponding wavelength.

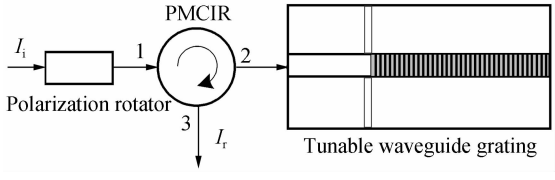

Fig. 1 Structure of the multi-parameter tunable filter

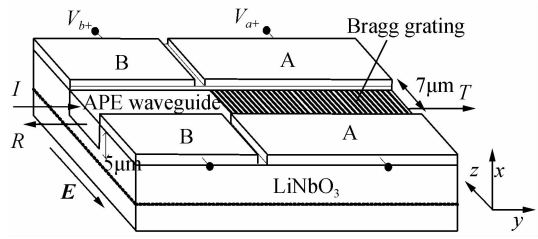

Fig. 2 Structure of the tunable waveguide grating

In our design, the gap of each electrodes pair is consistent with the width of the waveguide, and the electric field imposed by the electrodes parallel to *Z*-axis (optical axis) of the substrate. This layout not only improve the strength of $\boldsymbol{E}$, but also can use the largest EO coefficient of LN ($r_{33}=30.8$ pm/V), to maximize the tuning efficiency of the tunable waveguide grating.

2 Performance of the filter

2.1 Filtering performance

The filtering performance is determined by the Bragg grating, which obtained by periodic perturbation of thickness. According to waveguide grating transfer matrix theory[12], the reflectivity of the waveguide Bragg grating is

$$R=\frac{k_c^2\sinh^2(sl_a)}{(\delta/\Lambda)^2\sinh^2(sl_a)+s^2\cosh^2(sl_a)} \tag{1}$$

Where l_a is the length of the Bragg grating, $\delta=m\pi-\Lambda\beta$ is the mismatching parameter, β is the propagation constant of the waveguide, Λ is the period of the grating, m is a positive integer number denoting the grating order. $k_c=k^2w\sin[\beta\Lambda(1-D)]/\beta^2\Lambda h_{\text{eff}}$ is the coupling coefficient that quantifies the strength of the grating, w is the etching depth, k is the vector of transverse wave in the waveguide, h_{eff} is the effective thickness of the waveguide, and D is defined as etching duty cycle($D=$ Etching area/Λ). $s=\sqrt{k_c^2-(\delta/\Lambda)^2}$ is the decoupling coefficient. The strongest efficient coupling occurs when Bragg condition is satisfied, and Bragg condition (phase matching condition) is given by

$$m\lambda_B=2n_{\text{eff}}\Lambda \tag{2}$$

From Eq. (2), the Bragg wavelength (λ_B) depends on the period of the grating (Λ) and the effective refractive index (n_{eff}) of the grating. Take $m=1$, for $w=100$ nm, $D=1/2$, $n_{\text{eff}}\approx2.1389$, the period of the grating $\Lambda=362.3$ nm is achieved at the wavelength around 1 550 nm.

The fundamental properties of the grating can be obtained. For example, the peak reflectivity is

$$R_{\max}=[\tanh(k_cl_a)]^2 \tag{3}$$

And the bandwidth between two zeros of the spectral response is

$$\Delta\lambda=\frac{\lambda^2}{\pi n_{\text{eff}}l_a}\sqrt{(k_cl_a)^2+\pi^2} \tag{4}$$

It is obvious that the spectral characteristics of waveguide Bragg grating is consistent with fiber Bragg grating, but the coupling coefficient of the grating depends on the etching depth w and the etching duty cycle D on the conditions of single-mode waveguide.

Reflectivity and bandwidth are two important parameters that represent the performance of filter. The effect of duty cycle D with different etching depths on reflectivity is shown in Fig. 3. It can be seen that the highest reflectivity is obtained at duty cycle $D=0.5$ for different etching depth. The effect of duty cycle is ignorable when the etching depth is $w\geqslant 120$ nm around $D=0.5$.

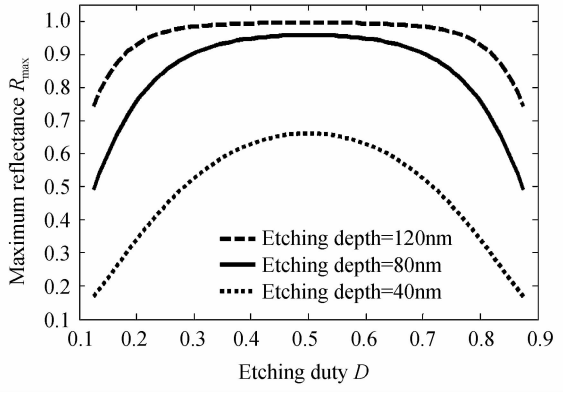

Fig. 3 Maximum reflectivity versus duty cycle D with different etching depth for $l=10.87$ mm

The relationship for max-reflectivity and bandwidth versus etching depth is shown in Fig. 4. It shows that the Max-reflectivity and bandwidth of the filter are both increased by enhancing the etching depth. The reflectivity of the filter R_{max} is around 98.6% with the corresponding bandwidth of 0.14 nm at the etching depth of 100 nm. When the etching depth is further enhanced, the improvement of reflectivity is not obvious, but bandwidth of the filter is increased obviously.

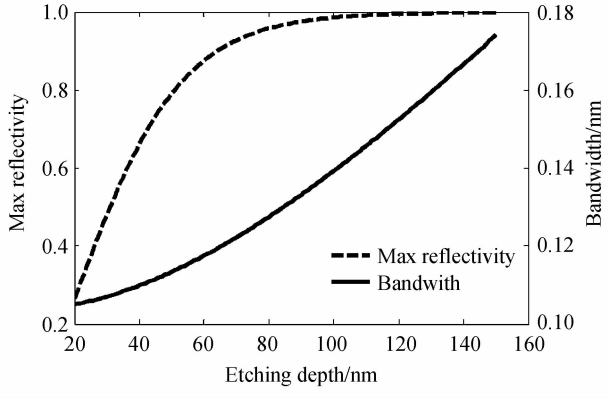

Fig. 4 Relationship for reflectivity and bandwidth versus etching depth with $D=0.5$, $l_a=10.87$ mm

Besides the grating parameters, applied voltage also affects the performance of the filter. As Fig. 5(a) shows that the maximum reflectivity of the filter decrease with voltage increasing. The slope of curve changes more obviously with the decrease of w, and the effect of voltage on the reflectivity can be ignored if the etching depth is large ($w\geqslant 120$ nm).

Fig. 5(b) indicates that increasing voltage will improve the narrow-band characteristic of the filter, and the impact of voltage is more obvious with larger w. Therefore, we should take advantage of applying positive voltage to improve the filtering performance.

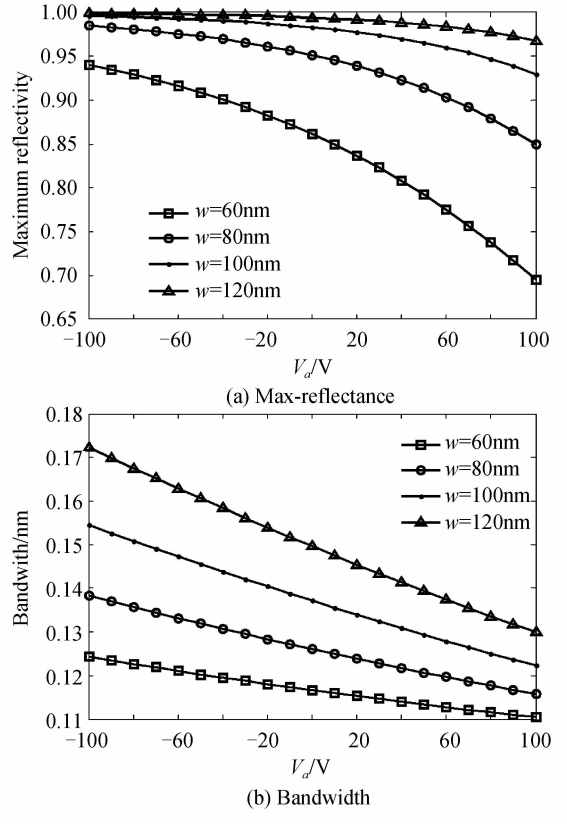

Fig. 5 The effect of the voltage (V_a) on filtering performance

2.2 Insertion loss

Insertion loss is an important performance index of the filter, in order to reduce the loss, an single-mode APE waveguides is designed based on the beam propagation method[13]. We get the single-mode waveguide with the width of 7 μm and the effective depth of 5 μm. The effective refractive index of the APE waveguide $N=2.139$ is also obtained at 1 550 nm.

The transverse mode field distribution of the waveguide is shown in Fig. 6, the mode field distribution is similar to the single-mode fiber's, and the horizontal and vertical mode field diameter are 10.56 μm and 7.22 μm respectively. The coupling loss is around 1.46 dB by computing the overlap integral of the transverse mode field of single-mode optical fiber and the waveguide.

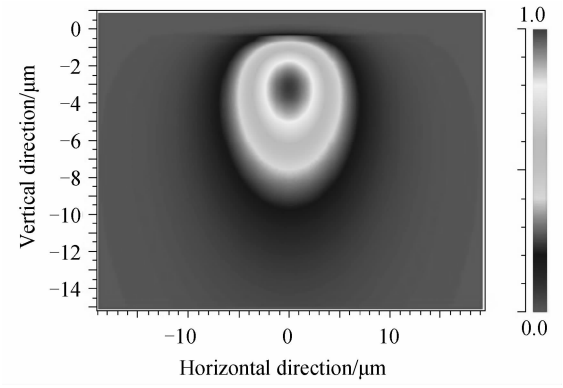

Fig. 6 Mode field distribution of APE single-mode waveguide

Insertion loss of the filter mainly includes the loss of the polarization rotator, the PMCIR and the tunable waveguide grating. The insertion of polarization rotator is about 1 dB, and generally, the loss of the PMCIR is low (≤0.8 dB). The loss of grating mainly comprises coupling loss and transmission loss, considering the propagation loss of the APE waveguide is very low (about 0.16 dB/cm)[14], the transmission loss of grating is about 0.464 dB with the waveguide length of 14.5 mm. Based on the above analysis, the insertion loss of the filter is about 3.7 dB.

3 Tuning analysis

3.1 Resonant wavelength tuning

The Bragg wavelength tuning of the filter is achieved in the tunable waveguide grating based on the $LiNbO_3$ EO effect. Electric field is imposed on electrodes A to change the refractive index of the waveguide and the Bragg wavelength is changed correspondingly according to Eq. (2). As a result, the spectral response of the Bragg grating can be shifted by the controlled voltage.

According to the theory of EO effect, for LN crystal, the applied electric field paralleling to the Z optical axis of crystal modifies the extraordinary refractive index (n) by an amount $\Delta n = r_{33} n^3 E/2$[8]. Combining Eq. (2), the tuning relationship between the wavelength λ_B and the applied voltage V_a is obtained

$$\Delta\lambda_B = r_{33} n_{eff}^3 \Lambda V_a / d \tag{5}$$

From the Eq. (5), the Bragg wavelength is tuned linearly by the applied voltage V_a. The tuning efficiency is around 15.6 pm/V considering the couple of electrodes with the gap of $d=7$ μm, and the central wavelength λ_B shifts to longer wavelength when increasing the voltage. In order to avoid the crystal polarization reversal caused by the high voltage, the applied voltage V_a should be controlled within −150 V～150 V. So we obtain that the maximum wavelength tuning range of the filter is about 4.68 nm.

Wavelength tuning speed of the filter is mainly decided by the response time of lithium niobate EO effect, and the tuning speed can reach the order of nm/ns[9], which is faster than other mechanisms.

3.2 Phase of λ_B tuning

The tuning of phase is also achieved by the way of electric control in the part of the tunable waveguide grating. The phase of λ_B is composed of reflected phase shift by the Bragg grating and propagation phase shift of APE waveguide without etching:

$$\varphi = \varphi_a + \varphi_b = \pi - \arctan\left[\frac{s\cosh(sl_a)}{\delta\sinh(sl_a)}\right] + 2\beta l_b \tag{6}$$

where φ_a is the reflected phase shift by the grating with the value of $-\pi/2$ at the wavelength λ_B, $\varphi_b = 2\beta l_b = 4\pi N l_b/\lambda_B$ is propagation phase shift of the APE waveguide, l_b is the length of APE waveguide without etching Bragg grating. Then Eq. (6) is simplified as

$$\varphi = -\pi/2 + 4\pi N l_b/\lambda_B \tag{7}$$

The relationship between the phase shift of and phase tuning voltage (V_b), with the length of the APE waveguide (l_b) 6 000Λ and 1 000Λ, is shown in Fig. 7, where φ means a relative phase shift quantity of λ_B between the input and output of the tunable Bragg grating, One φ-value corresponds to multiple V_b-values because of the periodicity of the phase, it is clear that the smallest V_b is the best choice. The figure shows that the phase tuning is linear with applied voltage. Increasing l_b will enhance the phase tuning efficiency, but also means the increase of the waveguide loss and the reduction in tuning precision. In our design, the phase tuning efficiency is 0.2π/V considering the APE waveguide with 3.623 mm length.

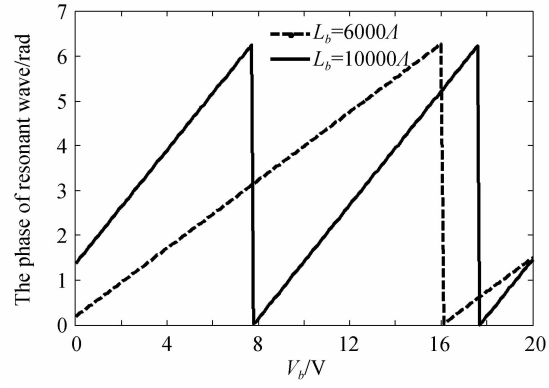

Fig. 7 Resonant wave phase tuning

Tuning mechanism of the phase is same as the wavelength tuning, and changing Bragg wavelength controlled by tuning voltage (V_a) does not affect the corresponding phase tuning efficiency, therefore, the phase can achieve real-time tuning with a high speed matching the tuning speed of the wavelength.

3.3 Intensity control

It well known that proton exchange makes extraordinary refractive index in the APE waveguide

increased, while ordinary refractive index decreased slightly, for a *Y*-propagating EM field in an *X*-cut crystal, only TE modes with polarization direction parallel to the *Z*-axis are permitted in the filter. With this feature, the control of intensity will be achieved by adjusting the angle between polarization of the light and the *Z*-axis of the substrate. The polarization rotator, which is consist of a polarizer and a half-wave plate, can realize the polarization direction control by adjusting the half-wave plate manually, and the polarization maintaining optical circulator is used to maintain the polarization of the light.

Intensity control is influenced by the input light polarization state. Considering the input light is linear polarization in the fiber, we should adjust the polarization direction of the polarizer consistent with the input light to avoid the loss of the light, and then adjust the half-wave plate to control the output light intensity. The control relationship is $I_R = \cos^2(\theta) I_I$, where θ is the angle between polarization direction of the light and *Z*-axis.

4 Conclusion

In this paper, a multi-parameter fast tunable Bragg grating filter on LN crystal has been proposed. The Bragg wavelength, the corresponding phase and the intensity of the filter are controlled independently. The wavelength and the phase are fast tunable in a linear way by the applied voltage with the wavelength tuning efficiency of 15.6 pm/V and the phase tuning efficiency of 0.2π/V, and the intensity control of the light is achieved by adjusting the polarization rotator. Numerical analysis found that the highest reflectivity is obtained at the duty cycle of 50% of the etched pattern, the coupling coefficient will be enhanced by increasing the etching depth, and the narrow-band feature of the filter can be increased by increasing the voltage. In addition, the filter also has advantages of fast tuning speed, high tuning efficiency, and low insertion loss (about 3.7 dB).

References

[1] DAS B K, SUCHE H, SHOLER W. Single-frequency Ti∶Er∶$LiNbO_3$ distributed Bragg reflector waveguide laser with thermally fixed photorefractive cavity[J]. *Applied Physics B*, 2001, **73**(5/6): 39-442.

[2] CHOI S, EOM T J, JUNG Y, *et al*. Broad-band tunable all-fiber band-pass filter based on hollow optical fiber and long-period grating pair[J]. *IEEE Photonics Technology Letters*, 2005, **17**(1): 115-117.

[3] KOCABAS A, AYDINLI A. Polymeric waveguide Bragg grating filter using soft lithography[J]. *Optics Express*, 2006, **14**(22): 10228-10232.

[4] LIU Qing, CHANG K S, LOR K P. Temperature sensitivity of a long-period waveguide grating in a channel waveguide gratings[J]. *Applied Physics Letters*, 2005, **86**(24): 241115 (1-3).

[5] CHU Y M, CHIANG K S, LIU Qing. Widely tunable optical band-pass filter by use of polymer long-period waveguide gratings[J]. *Applied Optics*, 2006, **45**(12): 2755-2760.

[6] GROBNIC D, MIHAILOV S J, SMELSER C W, *et al*. Bragg gratings made in reverse proton exchange lithium niobate waveguides with a femtosecond IR laser and a phase mask[J]. *IEEE Photonics Technology Letters*, 2005, **17**(7): 1453-1455.

[7] WANG Yi-ping, CHEN Jian-ping, LI Xin-wan, *et al*. Fast tunable electro-optic polymer waveguide gratings[J]. *Acta Physica Sinica*, 2005, **54**(10): 4782-4788.

[8] ARIZMENDI L. Photonic applications of lithium niobate crystals[J]. *Physic Status Solidi (a)*, 2004, 201(2): 253-283.

[9] PIERNO L, Dispenza M, SECCHI A. A lithium niobate electro-optic tunable Bragg filter fabricated by electron beam lithography[J]. *Journal of Optics A: Pure Applied Optics*, 2008, **10**(6): 064017-3.

[10] JIN Wei, CHIANG K S, LIU Q. Analysis of lithium niobate electrooptic long-period waveguide grating[J]. *Journal of Lightwave Technology*, 2010, **28**(10): 1477-1484.

[11] ZHANG Ai-ling, LI Chang-xiu. Dynamic optical arbitrary waveform generation with amplitude controlled by interference of two FBG arrays[J]. *Optics Express*, 2012, **20**(21): 23074-23081.

[12] CAO Zhuang-qi. The transfer matrix method of optical waveguide[M]. Shanghai: Shanghai Jiao Tong University Press, 2000.

[13] YEVICK D, HERMANSSON B. New formulations of the matrix beam propagation method: application to rib waveguides[J]. *IEEE Journal of Quantum Electronic*, 1989, **25**(2): 221-229.

[14] ZHANG De-long, DING Gui-lan, CUI Ming-yu, *et al*. Proton exchanged $LiNbO_3$ optical waveguide[J]. *Progress in Physics*, 2001, **2**(1): 45-65.